Metal-Metal-to-Ligand Charge Transfer Excited State and Supramolecular Polymerization of Luminescent Pincer Pd(II)-Isocyanide Complexes

*Qingyun Wan, Wai-Pong To, Chen Yang, and Chi-Ming Che**

Abstract: *Here are described pincer Pd^{II}-isocyanide complexes which display intermolecular interactions and emissive ^{3}MMLCT excited states in aggregation state(s) at room temperature. The intermolecular Pd^{II}-Pd^{II} and ligand-ligand interactions drive these complexes to undergo supramolecular polymerization in a living manner. Comprehensive spectroscopic studies reveal a pathway with a kinetic trap that can be modulated by changing the counter-anion and metal atom. The Pd^{II} supramolecular assemblies comprise two different aggregation forms with only one to be emissive. DFT/TDDFT calculations lend support to the MMLCT absorption and emission of these pincer Pd^{II}-isocyanide aggregates.*

Closed shell interactions between d^8 and/or d^{10} metal ions are appealing driving forces for self-assembly of supramolecular/polymeric systems, such as that of Pt^{II} and Au^{I}, having luminescent properties distinctly different from monomer counterparts,[1-3] as well as for self-assembly of anisotropic nanomaterials[4] or living supramolecular polymerization.[5,6] Incorporating metal-metal interaction into excited states, such as the ^{3}MMLCT (metal-metal-to-ligand charge transfer) ones of d^8 metal-organic supramolecular assemblies, would facilitate radiative decay of triplet excited state to ground state due to increased metal parentage in the frontier MOs.[7] This is particularly important in the design of new classes of luminescent Pd^{II} materials having fast k_r (radiative decay rate constant) as the emissive excited states of Pd^{II} monomer complexes are usually ^{3}IL (triplet intraligand) in nature with very long emission lifetimes. Over the past decades, considerable efforts have been directed to uncover Pd^{II}-Pd^{II} interactions and metal-metal bonded excited states of luminescent Pd^{II} complexes. While DFT calculations[8] and/or X-ray crystal structures[8d,9] lend evidence to the presence of Pd^{II}-Pd^{II} interactions, spectroscopic evidences for MMLCT and/or 4dσ*5pσ excited states attributable to Pd^{II}-Pd^{II} interactions remain elusive[10] as the Pd^{II}-Pd^{II} interaction is considerably weaker than the Pt^{II}-Pt^{II} one and Pd^{II} 4d orbitals are much lower in energy.[8a,11] In this work, we provide compelling evidence that pincer Pd^{II}-isocyanide complexes display intense ^{1}MMLCT absorption and emissive ^{3}MMLCT excited state upon supramolecular polymerization. In addition, the Pd^{II} complexes we report herein, and a Pt^{II} counterpart thereof, undergo supramolecular polymerization in a living manner. Fernández and co-workers reported cooperative supramolecular polymerization process of an oligophenyleneethynylene-based Pd^{II} pyridyl complex and Pd^{II}-Pd^{II} metallophilic interaction was suggested.[8c]

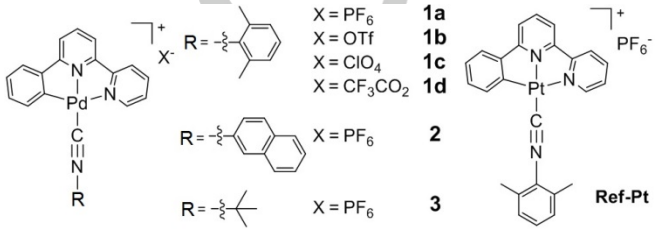

Scheme 1. Chemical structures of Pd^{II} and Pt^{II} complexes.

The details of synthesis and spectroscopic characterization of the Pd^{II} complexes **1**-**3** and **Ref-Pt** complex are provided in the Supporting Information. Complexes **1a**, **2** and **3** in CH_3CN show intense absorption bands at ~290-340 nm and 355-400 nm, which can be assigned to ^{1}IL and mixed ^{1}IL-^{1}MLCT transitions, respectively[12] (Figure S2). To induce the aggregation of the Pd^{II} complexes in solution, a H_2O/CH_3CN (9:1 v/v) solvent mixture was used. When H_2O (1800 μL) was injected into a CH_3CN solution (200 μL, 1×10^{-3} M) of **1a** or **1b**, an intense band at 439 nm developed for **1a**, while a broad, moderately intense band at 380 nm appeared for **1b** (Figure 1a,b). With increasing temperature, the peaks at 439 nm (**1a**) and 380 nm (**1b**) diminished gradually with a concomitant enhancement of absorption from the corresponding monomeric species. As revealed by the TDDFT calculations discussed later, the 380 and 439 nm peaks are attributed to ^{1}[π-π*] and ^{1}MMLCT excited states of the aggregation species, respectively. Upon lowering the temperature, spectroscopic changes for **1a** and **1b** (insets in Figure 1a,b) were distinctly different. For **1b**, a sigmodal curve is well fitted upon plotting the absorbance at 380 nm vs. temperature (Figure S7), suggesting an isodesmic mechanism for the oligomerization. For **1a**, upon lowering the temperature from 353 K to 318 K, a gradual increase in the absorption at 380 nm (inset i. in Figure 1a) was observed. Meanwhile, the changes in absorbance at 439 nm in this temperature range are indicative of a disfavored nucleation step followed by a highly favored elongation process at < 318 K (inset ii. in Figure 1a).[13]

A living supramolecular polymerization process was revealed by fast injection of H_2O into a CH_3CN solution of **1a** (Figure 1c). For molecular aggregation in a controlled living manner, there is a kinetically trapped state[14] which would prevent spontaneous nucleation and help to induce out-of-equilibrium self-assemblies.[15] A kinetically trapped metastable state of **1a** was observed, as evidenced by the lag time observed with [**1a**] = 5×10^{-5} M in Figure 1d. By changing the counter-anion from PF_6^- (**1a**) to OTf^- (**1b**), there was an immediate increase in absorbance at 380 nm after injection of H_2O, which remained little change with time. It indicated the absence of a kinetic trap in the aggregation pathway (supramolecular polymerization/oligomerization) for **1b**.

[*] Q. Wan, Dr. W.-P. To, Dr. C. Yang, Prof. Dr. C.-M. Che
State Key Laboratory of Synthetic Chemistry
Institute of Molecular Functional Materials
Department of Chemistry, The University of Hong Kong
Pokfulam Road, Hong Kong SAR, China.
E-mail: cmche@hku.hk

Prof. Dr. C.-M. Che
HKU Shenzhen Institute of Research and Innovation
Shenzhen, Guangdong, 518053, China

Supporting information for this article is given via a link at the end of the document.

We noticed that for **1a**, with the transformation from the kinetically trapped state to the aggregation state that showed ^{1}MMLCT absorption at 439 nm, an enhanced emission band at 540 nm developed (Figure 1e), while no emission was observed for **1b**. The supramolecular polymerization was faster for Pt^{II} analogue (10 min for Pd^{II} and 7 min for Pt^{II} at 5×10^{-5} M to attain a maximum value of absorbance due to the aggregates). For the **Ref-Pt** complex, upon injecting H_2O into its CH_3CN solution (Figure 1f), a distinct band at 579 nm gradually developed with a slight decrease of the absorption at 440 nm. In addition, the total concentration of **1a**, **1c** or **Ref-Pt** in the mixed solvent could affect the oligomerization pathway (Figure 1d, Figure S9). As an example, the time required for the 439 nm absorbance to attain a maximum value decreased as the total concentration of **1a** increased. With regard to the aforementioned time-dependent absorption spectral changes, we suggest that **1a**, **1c** and **Ref-Pt** underwent supramolecular polymerization in a living manner with an aggregation pathway that can be modulated by the counter-anion.

The crystal structure of **1a** shows an infinite Pd^{II}-Pd^{II} chain featuring Pd^{II}-Pd^{II} distance of ~3.3–3.4 Å with its molecules arranged in alternately skewed and head-to-tail fashion; the counter-anion PF_6^- is remote from the 1D chain (Figure 2a). In contrast, the crystal structure of **1b** shows discrete cation pairs; the counter-anion OTf^- blocks Pd^{II}-Pd^{II} contact between neighboring cation pairs (Figure 2b) and displays close contact (3.25 Å) with the pyridyl ring of the Pd^{II} complex. Based on these structural data, an energy landscape could be constructed (Figure 2c), wherein aggregation species composed of counter-anion-blocked cation pairs and 1D chains are termed “aggregate 1” (Agg1) and “aggregate 2” (Agg2), respectively. Agg1 can be regarded as a kinetic trap out of the thermodynamic equilibrium in the supramolecular polymerization. Thus, **1a** initially aggregated to form Agg1, which, upon breaking the Pd^{II} cation-PF_6^- interaction, subsequently transformed to Agg2. For **1b**, aggregation stopped at Agg1 state attributable to the Pd^{II} cation-OTf^- interaction. Interestingly, a slow polymerization process was observed for **1c** (counter-anion: ClO_4^-), which took 1 day to produce a slight increase in absorbance of the 439 nm band, indicating a considerably retarded formation of Agg2 (Figure S8). Complex **1d** (counter-anion: $CF_3CO_2^-$), like **1b**, showed no living supramolecular polymerization. Theoretical study on anion-π interactions showed that among all the anions calculated, PF_6^- shows the weakest anion-π interaction due to the lack of effective electrostatic interaction.[16]

The driving force for the supramolecular polymerization to give Agg2 state comes from the attractive interactions between the complex cations. Based on theoretical studies, “cation-cation” attractive interactions can be accounted for by dispersive interactions.[17] For **2** and **3**, both ^{1}MMLCT absorption and living supramolecular polymerization were not observed. Presumably the π-π interactions between napthyl units (**2**) and steric effect of *tert*-butyl groups (**3**) disfavor close Pd^{II}-Pd^{II} contact and hence formation of a Pd^{II}-Pd^{II} chain.

DFT/TDDFT calculations were performed on **1** and oligomers $[\mathbf{1}]_n$ (n = 2–4), with initial guess of geometry from X-ray crystal structures, to investigate the electronic structures of the cation pairs (n = 2, **1b**) and 1D oligomer chain (n: limited to 4 due to computation constraints, **1a**), respectively. Water is chosen as the solvent for calculation as aggregation takes place upon addition of water. The DFT optimized structure of $[\mathbf{1}]_4$ features alternately skewed and head-to-tail arrangement (C(C≡N)-Pd-Pd-C(C≡N) torsion angles: 111.9° and 177.5°) reminiscent of the X-ray crystal structure (corresponding torsion angles: 113.7° and 180.0°). As revealed by the MOs diagrams (Figure 3), for dimer $[\mathbf{1}]_2$, the antibonding $\sigma^*(4d_{z^2})$ orbital becomes H-2; the splitting between two $4d_{z^2}$ orbitals is not sufficient to make $\sigma^*(4d_{z^2})$ orbital

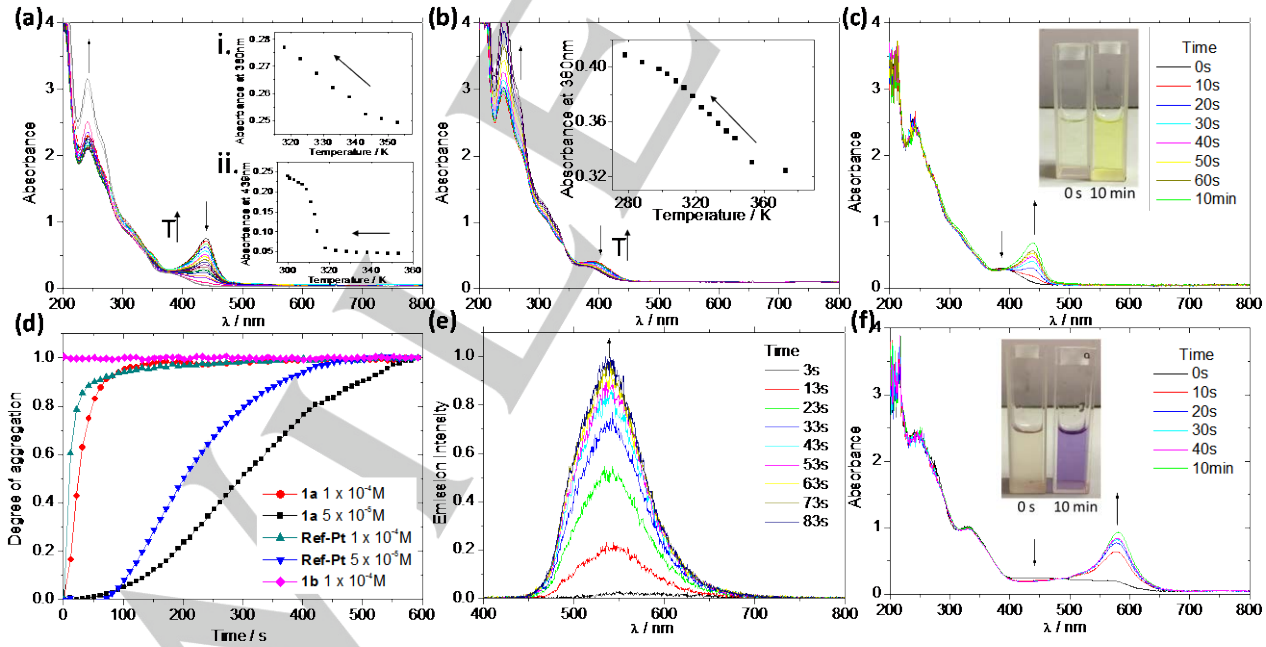

Figure 1. (a) Temperature-dependent UV/Vis absorption spectra of **1a** (1×10^{-4} M) in H_2O/CH_3CN (9:1 v/v) from 298 K to 343 K; insets: changes of absorbance at 380 nm (i) and 439 nm (ii) upon lowering temperature. (b) Temperature-dependent UV/Vis absorption spectra of **1b** (1×10^{-4} M) in H_2O/CH_3CN (9:1 v/v) from 273 K to 373 K; inset: change of absorbance at 380 nm upon lowering temperature. (c) Time-dependent absorption spectral changes of **1a** (1×10^{-4} M) at 298 K (0 s: immediately after injection of H_2O); inset: corresponding color changes recorded at the indicated times. (d) Time-dependent degree of aggregation of **1a**, **1b** and **Ref-Pt**, calculated from the absorbance at 439 nm for **1a**, 380 nm for **1b**, 579 nm for **Ref-Pt** at the indicated concentration at 298 K. (e) Time-dependent emission spectral changes of **1a** (1×10^{-4} M) at 298 K. (f) Time-dependent absorption spectral changes of **Ref-Pt** at 298 K; inset: color changes recorded at the indicated time.

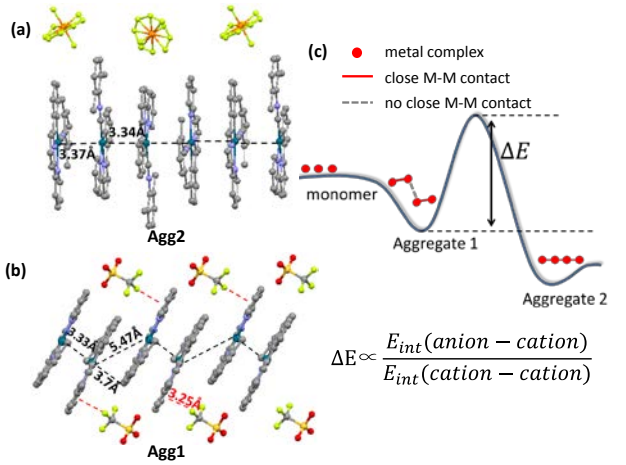

Figure 2. (a) Crystal structure of **1a** featuring a 1D infinite structure with a Pd^{II}-Pd^{II} chain. (b) Crystal structure of **1b** highlighting the cation pair features. Hydrogen atoms are omitted for clarity. (c) Qualitative energy landscape of supramolecular polymerization models with a competing kinetic stabilization state.

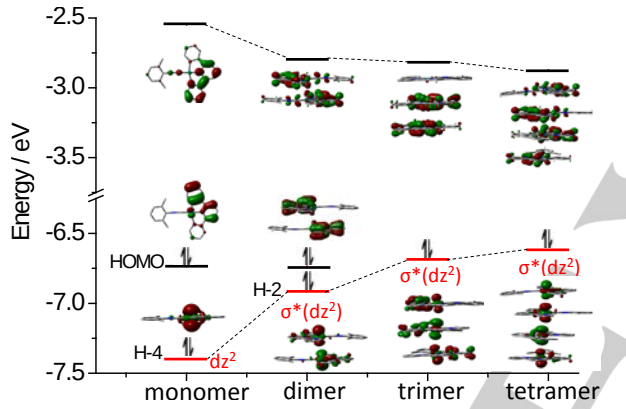

Figure 3. Calculated MOs diagrams of **1** and oligomers $[\mathbf{1}]_n$ (n = 2–4).

become HOMO. When n increases to 3, the σ*($4d_{z^2}$) orbital becomes HOMO. Meanwhile, the LUMO (composed of π-localized orbitals from the C^N^N ligands) is stabilized upon oligomerization because of enhanced π-π stacking interaction. The HOMO-LUMO gap further decreases when the oligomer chain elongates to n = 4. Excitation of an electron from σ*($4d_{z^2}$) orbital (HOMO) to the ligand-localized LUMO gives rise to ^{1}MMLCT transition which appears as an intense absorption band at 439 nm for the Agg2 state of **1a**. The TDDFT calculated UV/Vis absorption spectra (Figure S16) show a moderately intense band at ~390 nm for $[\mathbf{1}]_2$ (attributable to the ^{1}[π-π*] transition; match the experimentally observed 380 nm band in Figure 1b) and an intense red-shifted band at ~424 nm for $[\mathbf{1}]_4$ (with close Pd^{II}-Pd^{II} contacts) reminiscent of the ^{1}MMLCT absorption band at 439 nm depicted in Figure 1a.

Photo-physical properties of the emissive aggregates of **1a** monitored at λ_{max} 540 nm were examined at different time intervals. According to the quantum yield and lifetime calculated for the 540 nm emission where there was no further increase in intensity (attributed to the complete transformation to Agg2) (Figure 4b), the k_r was calculated to be 62.2×10^4 s^{-1}. A large k_r was also found for the ^{3}MMLCT emission of **Ref-Pt** aggregate(s) (k_r 109.2×10^4 s^{-1}; λ_{max} 720 nm; τ 0.12 μs; ϕ 13.1 %; concentration 1×10^{-4} M; H_2O/CH_3CN 9:1 v/v) which is over 22-fold higher than that of the emission of monomeric **Ref-Pt** (k_r 4.8×10^4 s^{-1};

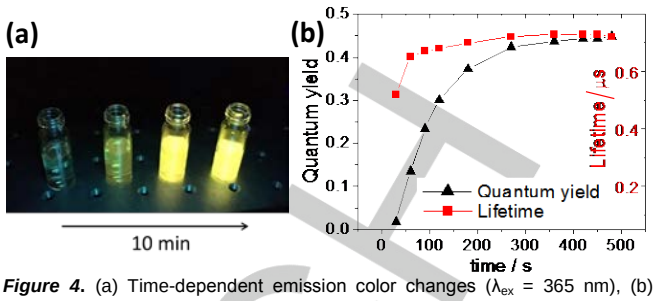

Figure 4. (a) Time-dependent emission color changes (λ_{ex} = 365 nm), (b) time-dependent emission quantum yield (black line) and lifetime (red line) at λ_{em} = 540 nm of **1a** at 298 K upon injecting H_2O (2700 μL) into the CH_3CN solution (300 μL, 1×10^{-3} M).

λ_{max} 525 nm; τ 0.33 μs; ϕ 1.6 %; concentration 1×10^{-4} M; H_2O/CH_3CN 0:100 v/v).

The difference in luminescent properties between Agg2 and Agg1 states can be attributed to their electronic configurations. As depicted in Figure 3, both HOMO and LUMO of the dimer (cation pair, Agg1) are localized on the C^N^N ligands, while the HOMO of the tetramer (1D oligomer, Agg2) is largely composed of Pd ($4d_{z^2}$) orbitals. Upon light excitation, Agg2, with a greater metal parentage in the frontier MOs, would display a larger SOC (spin orbital coupling) effect,[18] leading to faster radiative decay from the triplet excited state to singlet ground state. It is worth noting that the k_r values for Agg2 of **1a** (62.2×10^4 s^{-1}) is substantially higher than that of the reported Pd^{II} complexes with emission from ligand-localized excited state (k_r ~ 10^3 s^{-1}).[19] This finding indicates that the 540 nm emission of **1a** in Agg2 state should not be ^{3}IL in nature and is assigned to ^{3}MMLCT excited state. TDDFT calculations revealed shortening of Pd-Pd distance at triplet excited state T_1 for tetramer $[\mathbf{1}]_4$ (Figure S18a). The emission wavelength of $[\mathbf{1}]_4$ was calculated to be 583 nm with the transition from σ*($4d_{z^2}$) (HOMO) to LUMO having C^N^N ligand character (Figure S18b), which is consistent with the experimentally observed 540 nm emission of **1a** in Agg2 attributable to ^{3}MMLCT excited state.

SEM images showed the formation of nanowires of **1a** in H_2O/CH_3CN (9:1 v/v), unlike the nanoparticles formed in the solutions of **1b** and **1d** (Figure S4). This suggests that **1a** followed a different self-assembly pathway compared to **1b** and **1d** (note the different spectroscopic changes between **1a** and **1b**). The construction of 1D oligomers with a linear Pd^{II}-Pd^{II} chain is considered to be critically important for the formation of nano-wire structure.

For **1c**, the relatively slow oligomerization to Agg2 state prompted us to use a seeded supramolecular polymerization approach to facilitate its growth.[5,6,15,20] Addition of **1a**-Agg2 (1800 μL, 1×10^{-5} M) to a CH_3CN solution of **1c** (200 μL, 1×10^{-3} M) led to transformation of Agg1 to Agg2 within 1 h (Figure 5b). The absence of a lag time (Figure 5b, inset) is supportive of an externally seeded growth assembly of Agg2. A step-growth mechanism for the seed-catalyzed supramolecular polymerization is depicted in Figure 5a. We propose that the **1a**-Agg2 weakened the Pd^{II} cation-ClO_4^- interaction by generating competing cation-cation dispersive interactions, thereby facilitating elongation of the oligomers. Figure 5d,e show the morphology of supramolecular polymers obtained at 30 min and 60 min after injecting the **1a**-Agg2 to **1c** solution, respectively. The elongation of the polymer shown in Figure 5e is indicative of a step-growth mechanism. We also found that the oligomerization kinetics can be modulated by the concentration of externally added seeds (Figure S19).

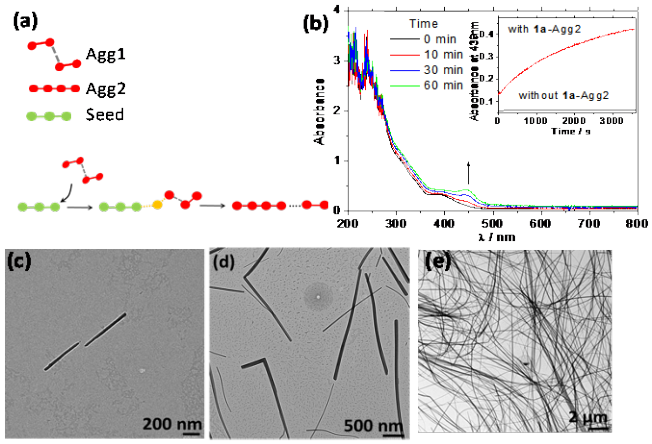

Figure 5. (a) Schematic representation of the seeded supramolecular polymerization process. (b) Time-dependent absorption spectra of **1c** with the aid of **1a**-Agg2 (ratio of **1c** to **1a**-Agg2: 11:1); inset: time-dependent absorbance change at 439 nm for **1c** with and without **1a**-Agg2. (c) TEM image of **1a**-Agg2 (1×10^{-5} M). (d) and (e) Time-dependent TEM images of **1c** with the aid of **1a**-Agg2 (1×10^{-5} M) obtained at 30 and 60 min, respectively.

In conclusion, we have demonstrated the modulation of living supramolecular polymerization for d^8 Pd^{II} complexes by tuning the "cation-anion" electrostatic and "cation-cation" dispersive interactions. Our study reveals that the pincer Pd^{II} complexes display $^{1/3}$MMLCT absorption and emission in the visible spectral region. The enhanced SOC and hence increased k_r value account for the switch-on of ^{3}MMLCT emission of pincer Pd^{II} aggregates.

Acknowledgements

This work was supported by the Area of Excellence Program (AoE/P-03/08), the National Key Basic Research Program of China (No. 2013CB834802), the Hong Kong Research Grants Council (HKU 17300614) and Basic Research Program of Shenzhen (JCYJ20160229123546997, JCYJ20160530184056496). This work was also conducted in part using the research computing facilities and/or advisory services offered by Information Technology Services, The University of Hong Kong. We thank Dr. K.-H. Low for assistance in solving the X-ray crystal structures of **1b** and **3**.

Keywords: palladium • living supramolecular polymerization • MMLCT • intermolecular interaction

[1] P. Pyykkö, *Chem. Rev.* **1997**, *97*, 597.
[2] a) D. M. Roundhill, H. B. Gray, C.-M. Che, *Acc. Chem. Res.* **1989**, *22*, 55; b) W. Lu, K. T. Chan, S.-X. Wu, Y. Chen, C.-M. Che, *Chem. Sci.* **2012**, *3*, 752; c) V. W.-W. Yam, V. K.-M. Au, S. Y.-L. Leung, *Chem. Rev.* **2015**, *115*, 7589; d) A. Aliprandi, D. Genovese, M. Mauro, L. De Cola, *Chem. Lett.* **2015**, *44*, 1152; e) K. Li, G. S. M. Tong, Q. Wan, G. Cheng, W.-Y. Tong, W.-H. Ang, W.-L. Kwong, C.-M. Che, *Chem. Sci.* **2016**, *7*, 1653.
[3] a) H. Yersin, G. Gliemann, *Ann. N.Y. Acad. Sci.* **1978**, *313*, 539; b) H.-K. Yip, C.-M. Che, Z.-Y. Zhou, T. C. Mak, *J. Chem. Soc., Chem. Commun.* **1992**, 1369; c) S.-W. Lai, M. C.-W. Chan, T.-C. Cheung, S.-M. Peng, C.-M. Che, *Inorg. Chem.* **1999**, *38*, 4046; d) M. Han, Y. Tian, Z. Yuan, L. Zhu, B. Ma, *Angew. Chem.* **2014**, *126*, 11088; *Angew. Chem. Int. Ed.* **2014**, *53*, 10908; e) M. R. R. Prabhath, J. Romanova, R. J. Curry, S. R. P. Silva, P. D. Jarowski, *Angew. Chem.* **2015**, *127*, 8060; *Angew. Chem. Int. Ed.* **2015**, *54*, 7949.
[4] a) W. Lu, V. A. L. Roy, C.-M. Che, *Chem. Commun.* **2006**, 3972; b) Y. Sun, K. Ye, H. Zhang, J. Zhang, L. Zhao, B. Li, G. Yang, B. Yang, Y. Wang, S.-W. Lai, C.-M. Che, *Angew. Chem.* **2006**, *118*, 5738; *Angew. Chem. Int. Ed.* **2006**, *45*, 5610; c) M.-Y. Yuen, V. A. L. Roy, W. Lu, S. C. F. Kui, G. S. M. Tong, M.-H. So, S. S.-Y. Chui, M. Muccini, J. Q. Ning, S. J. Xu, C.-M. Che, *Angew. Chem.* **2008**, *120*, 10043; *Angew. Chem. Int. Ed.* **2008**, *47*, 9895; d) Y. Chen, K. Li, W. Lu, S. S.-Y. Chui, C.-W. Ma, C.-M. Che, *Angew. Chem.* **2009**, *121*, 10093; *Angew. Chem. Int. Ed.* **2009**, *48*, 9909; e) C. Po, A. Y.-Y. Tam, K. M.-C. Wong, V. W.-W. Yam, *J. Am. Chem. Soc.* **2011**, *133*, 12136; f) H.-L. Au-Yeung, S. Y.-L. Leung, A. Y.-Y. Tam, V. W.-W. Yam, *J. Am. Chem. Soc.* **2014**, *136*, 17910; g) S. Y.-L. Leung, K. M.-C. Wong, V. W.-W. Yam, *Proc. Natl. Acad. Sci. U. S. A.* **2016**, *113*, 2845.
[5] a) M. E. Robinson, D. J. Lunn, A. Nazemi, G. R. Whittell, L. De Cola, I. Manners, *Chem. Commun.* **2015**, *51*, 15921; b) M. E. Robinson, A. Nazemi, D. J. Lunn, D. W. Hayward, C. E. Boott, M.-S. Hsiao, R. L. Harniman, S. A. Davis, G. R. Whittell, R. M. Richardson, L. De Cola, I. Manners, *ACS Nano* **2017**, *11*, 9162.
[6] A. Aliprandi, M. Mauro, L. De Cola, *Nat. Chem.* **2016**, *8*, 10.
[7] a) Q. Wang, I. W. H. Oswald, X. Yang, G. Zhou, H. Jia, Q. Qiao, Y. Chen, J. Hoshikawa-Halbert, B. E. Gnade, *Adv. Mater.* **2014**, *26*, 8107; b) Y. Guo, L. Xu, H. Liu, Y. Li, C.-M. Che, Y. Li, *Adv. Mater.* **2015**, *27*, 985; c) K. T. Ly, R.-W. Chen-Cheng, H.-W. Lin, Y.-J. Shiau, S.-H. Liu, P.-T. Chou, C.-S. Tsao, Y.-C. Huang, Y. Chi, *Nat. Photonics* **2017**, *11*, 63.
[8] a) B.-H. Xia, C.-M. Che, Z.-Y. Zhou, *Chem. Eur. J.* **2003**, *9*, 3055; b) J. Luo, J. R. Khusnutdinova, N. P. Rath, L. M. Mirica, *Chem. Commun.* **2012**, *48*, 1532; c) M. J. Mayoral, C. Rest, V. Stepanenko, J. Schellheimer, R. Q. Albuquerque, G. Fernández, *J. Am. Chem. Soc.* **2013**, *135*, 2148; d) I. Mitra, G. K. Ghosh, S. Mukherjee, V. P. Reddy B., W. Linert, F. Kubel, X. Rocquefelte, S. C. Moi, *Polyhedron* **2015**, *89*, 101.
[9] a) T. Tu, W. Assenmacher, H. Peterlik, R. Weisbarth, M. Nieger, K. H. Dötz, *Angew. Chem.* **2007**, *119*, 6486; *Angew. Chem. Int. Ed.* **2007**, *46*, 6368; b) I. M. Sluch, A. J. Miranda, O. Elbjeirami, M. A. Omary, L. M. Slaughter, *Inorg. Chem.* **2012**, *51*, 10728; c) X. Yin, S. A. Warren, Y.-T. Pan, K.-C. Tsao, D. L. Gray, J. Bertke, H. Yang, *Angew. Chem.* **2014**, *126*, 14311; *Angew. Chem. Int. Ed.* **2014**, *53*, 14087.
[10] M. D. Santana, L. López-Banet, G. Sánchez, J. Pérez, E. Pérez, L. García, J. L. Serrano, A. Espinosa, *Dalton Trans.* **2016**, *45*, 8601.
[11] a) S.-W. Lai, T.-C. Cheung, M. C. W. Chan, K.-K. Cheung, S.-M. Peng, C.-M. Che, *Inorg. Chem.* **2000**, *39*, 255; b) W. Lu, M. C. W. Chan, N. Zhu, C.-M. Che, C. Li, Z. Hui, *J. Am. Chem. Soc.* **2004**, *126*, 7639; c) J. E. Bercaw, A. C. Durrell, H. B. Gray, J. C. Green, N. Hazari, J. A. Labinger, J. R. Winkler, *Inorg. Chem.* **2010**, *49*, 1801; d) N. Marino, C. H. Fazen, J. D. Blakemore, C. D. Incarvito, N. Hazari, R. P. Doyle, *Inorg. Chem.* **2011**, *50*, 2507; e) I. Georgieva, N. Trendafilova, N. I. Dodoff, *J. Photochem. Photobiol., A* **2013**, *267*, 35.
[12] S.-W. Lai, H.-W. Lam, W. Lu, K.-K. Cheung, C.-M. Che, *Organometallics* **2002**, *21*, 226.
[13] M. M. J. Smulders, M. M. L. Nieuwenhuizen, T. F. A. de Greef, P. van der Schoot, A. P. H. J. Schenning, E. W. Meijer, *Chem. Eur. J.* **2010**, *16*, 362.
[14] F. Würthner, *Nat. Chem.* **2014**, *6*, 171.
[15] M. Endo, T. Fukui, S. H. Jung, S. Yagai, M. Takeuchi, K. Sugiyasu, *J. Am. Chem. Soc.* **2016**, *138*, 14347.
[16] J. Xi, X. Xu, *Phys. Chem. Chem. Phys.* **2016**, *18*, 6913.
[17] S. Grimme, J.-P. Djukic, *Inorg. Chem.* **2011**, *50*, 2619.
[18] a) G. S.-M. Tong, C.-M. Che, *Chem. Eur. J.* **2009**, *15*, 7225; b) G. S. M. Tong, P. K. Chow, W.-P. To, W.-M. Kwok, C.-M. Che, *Chem. Eur. J.* **2014**, *20*, 6433.
[19] P.-K. Chow, G. Cheng, G. S. M. Tong, C. Ma, W.-M. Kwok, W.-H. Ang, C. Y.-S. Chung, C. Yang, F. Wang, C.-M. Che, *Chem. Sci.* **2016**, *7*, 6083.
[20] a) D. Colombani, *Prog. Polym. Sci.* **1997**, *22*, 1649; b) S. Ogi, V. Stepanenko, J. Thein, F. Würthner, *J. Am. Chem. Soc.* **2016**, *138*, 670.

Entry for the Table of Contents

COMMUNICATION

Here are described pincer Pd^{II}-isocyanide complexes which display intermolecular interactions and emissive ^{3}MMLCT excited states in aggregation form(s) at room temperature. The Pd^{II} supramolecular assemblies comprise two different aggregation states with only one to be emissive.

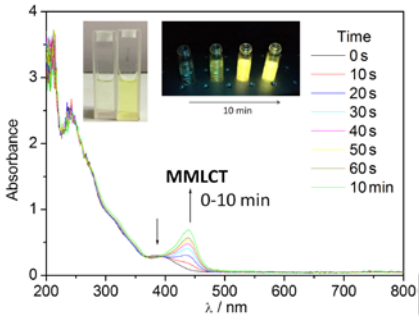

Qingyun Wan, Wai-Pong To, Chen Yang, and Chi-Ming Che*

Page No. – Page No.

Metal-Metal-to-Ligand Charge Transfer Excited State and Supramolecular Polymerization of Luminescent Pincer Pd(II)-Isocyanide Complexes